



## SHEAR DEFORMATION MODELS FOR LARGE-STRAIN SHELL ANALYSIS

Y. BAŞAR and Y. DING

Institut für Statik und Dynamik, Ruhr-Universität Bochum, Germany

(Received 20 December 1995; in revised form 26 May 1996)

**Abstract**—The objective is the theoretical and numerical simulation of large-strain phenomena of rubber-like shells by means of shear deformation models. The development starts with a general applicable shell model constructed on the basis of a quadratic displacement approximation which involves two thickness stretching parameters. This model is then coupled with incompressible material models of Mooney–Rivlin and neo-Hookean types. Material incompressibility is described by two-dimensional constraints considered at the element level as subsidiary conditions. A special care is given to the stress prediction in the presence of large-strains. After transformation of the theoretical model into an incremental formulation a four-node isoparametric finite element is derived. Examples are finally given to demonstrate the ability of this model to deal with very strong deformations and to predict the related stresses. © 1997 Elsevier Science Ltd.

### 1. INTRODUCTION

Shells composed particularly of rubber-like materials are very flexible structures able to perform, besides finite rotations, large strains. Finite rotation phenomena are characterized by very large rotations of the shell director while thickness changes are supposed to be negligible during the deformation process. A lot of works have been dedicated in the last decade to the computer simulation of finite rotations. Thus a large number of efficient finite rotation models [see Simo *et al.* (1989, 1990a); Gruttmann *et al.* (1989); Gebhardt (1990); Başar and Ding (1990); Büchter and Ramm (1992); Sansour and Bufler (1992); Başar *et al.* (1992)] are now available, developed according to various approaches. Attention has also been given to the inclusion of transverse normal strains [see Kühllhorn and Schoop (1992); Simo *et al.* (1990b); Büchter *et al.* (1994); Başar and Ding (1994); Sansour (1995)] and the twisting degrees of freedom [see Fox and Simo (1992); Simo (1993); Ibrahimbegovic and Frey (1994)], the last aspect being relevant for the analysis of shells with geometry intersections.

After all these developments the question now arises what is to be achieved additionally to simulate structures with large strains. This question will be treated here primarily for rubber-like shells characterized by material incompressibility starting however from a general applicable kinematic model. Here we emphasize that, in geometrical sense, large-strain phenomena are characterized by significant thickness changes. Evidently, such deformations may involve also finite rotations, which are understood to be an accompanying effect of large strains. Now the question is, how to proceed to simulate shells with large strains? Research aspects being relevant for the treatment of this topic cover: the inclusion of transverse normal strains  $\gamma_{33}$  by a suitable kinematic model, the consideration of the incompressibility condition and a consistent two-dimensional modeling of strain energy density, the last two aspects being closely related to modeling of the material behavior.

We now deal with the first aspect. In classical shell models [Başar and Krätzig (1985)] the deformed shell continuum  $\mathbf{r}^*(\theta^i)$  is described by a linear expression in thickness coordinate  $\theta^3$  postulating, in addition, an inextensible director  $\mathbf{d}_3$

$$\mathbf{r}^* = \mathbf{r} + \theta^3 \mathbf{d}_3, \quad \mathbf{d}_3 \cdot \mathbf{d}_3 = 1 \rightarrow \text{M5.}$$

This model with five independent parameters (M5) implies the vanishing of transverse normal strains  $\gamma_{33}$ . Many efforts have been devoted to the extension of the classical shear

deformation model (M5) to consider the thickness changes [see Lo *et al.* (1977); Kühlnhorn and Schoop (1992); Sansour (1995)]. To take account for  $\gamma_{33}$  the above expression is to be augmented at least by a single stretching parameter  $\lambda$  to be considered for numerical convenience [Simo *et al.* (1990b), Başar and Ding (1994)] through a multiplicative decomposition as

$$\mathbf{r}^* = \mathbf{r} + \theta^3 \lambda \mathbf{d}_3, \quad \mathbf{d}_3 \cdot \mathbf{d}_3 = 1 \rightarrow \text{M6.}$$

The so resulting six parametric model performs very well for incompressible materials, but may lead to numerical difficulties when it is applied to compressible shells [see Büchter *et al.* (1994); Başar and Ding (1994)]. This deficiency disappears automatically if a quadratic stretching parameter  $\bar{u}_3$  is additionally considered:

$$\mathbf{r}^* = \mathbf{r} + \theta^3 (\lambda + \theta^3 \bar{u}_3) \mathbf{d}_3, \quad \mathbf{d}_3 \cdot \mathbf{d}_3 = 1 \rightarrow \text{M7.}$$

It is, of course, possible to use a vectorial quantity  $\mathbf{u} = \bar{u}_x \mathbf{a}^x + \bar{u}_3 \mathbf{d}_3$  as quadratic term leading to

$$\mathbf{r}^* = \mathbf{r} + \theta^3 \lambda \mathbf{d}_3 + (\theta^3)^2 \mathbf{u}, \quad \mathbf{d}_3 \cdot \mathbf{d}_3 = 1 \rightarrow \text{M9,}$$

but numerical studies on compressible structures [Başar and Ding (1994)] have shown that the inclusion of  $\bar{u}_x$  is irrelevant for a significant improvement of the analysis accuracy and superfluous concerning numerical stability. If the shell is incompressible and sufficiently thin, the analysis may be achieved even by the linear model M6 without significant loss of accuracy. Accordingly, also the third component  $\bar{u}_3$  turns out not to be of major importance for incompressible and thin shells. A further improvement of the kinematic approach is not of practical significance. This would lead to very complicated shell equations. On the other hand, it is well-known [Başar and Ding (1995)] that multilayer models based on a layerwise application e.g. of M6 are decisively superior to any refined single layer model concerning different aspects e.g. the prediction of stress concentrations. Finally, we cite the kinematic model due to Makowski and Stumpf (1989)

$$\mathbf{r}^* = \mathbf{r} + \theta^3 \lambda \mathbf{d}_3, \quad \mathbf{d}_3 \cdot \mathbf{d}_3 = 1 \rightarrow M^*$$

with a parameter  $\lambda = \lambda(\theta^1)$  where the role of transverse strains seems to be overestimated.

The kinematic models discussed above permit the consideration of shear deformations with different accuracy level. It is, of course, possible to use them, as is the case e.g. in Makowski and Stumpf (1989) and Başar and Ding (1995), by adopting the so-called extended Kirchhoff–Love hypothesis which implies a deformation behaviour depending solely upon the midsurface position vector  $\mathbf{r} = \mathbf{r}(\theta^z)$  for incompressible materials. The basic idea of this hypothesis is the neglect of the shear strains ( $\gamma_{z3} = 0$ ) while transverse normal strains  $\gamma_{33}$  are, in contrast to its classical version, considered.

Kirchhoff–Love type assumptions have been already used in the analysis of rubber-like shells to construct general applicable shell models [Makowski and Stumpf (1989)] and recently to achieve finite element formulations. A general applicable Kirchhoff–Love type model has been presented also in Schieck *et al.* (1992), where the theoretical formulation has been additionally transformed into an efficient triangular shell element. A particularity of the derivation is that two-dimensional (2D) strains are introduced directly by series expansions without introducing a kinematic approach. Displacement-based finite elements on the basis of general applicable shell theory have been also proposed later in Başar and Ding (1996). In contrast to Schieck *et al.* (1992) the development has been however achieved starting from a kinematic approach providing the consistency of 2D strain fields. In this work attention is also given for the calculation of the stresses.

Shear deformations  $\gamma_{z3}$  have been omitted in the above cited models. These deformations may however influence the response significantly for thick shells but particularly

for those consisting of dissimilar material layers. Shear deformation models are also attractive since they provide a more systematical finite element formulation. In the field of large strains shear deformations have been considered only in few theoretical formulations [see Taber (1985)] and very rarely in developing finite elements. From this overview it may be deduced that there is a serious lack of general applicable shear-deformation models on large-strain analysis of incompressible shells.

Rubber-like materials can be modelled like hyperelastic materials through the strain energy density. A formulation widely used for this purpose is the Mooney–Rivlin model involving the neo-Hookean model as a special case. These models have been already adopted in developing general applicable finite elements [Schiek *et al.* (1992); Bařar and Ding (1996)]. A further possibility is the use of Ogden model, which has been mainly employed in membrane shell models [Wriggers and Taylor (1990); Gruttman and Taylor (1992)]. A disadvantage of this model is the fact that it requires the transformation of the actual strains into principal stretches. The incorporation of the incompressibility condition into strain energy densities causes essentially no difficulties. The problem is the transformation of the resulting expressions into a consistent 2D formulation. Corresponding expressions can be found in Simmonds (1986) for axisymmetric deformations and in Schieck (1989), Bařar and Ding (1996) for arbitrary bending deformations.

The objective of this contribution is the development of a shear-deformation theory for large strain shell analysis and its transformation into a finite element mode. To achieve a formulation applicable both to compressible and incompressible materials the displacement field is described by a quadratic polynomial in thickness coordinate using a multiplicative decomposition for the first order term. This kinematic model is then applied to rubber-like shells simulating the material behavior by Mooney–Rivlin and neo-Hookean models. The incompressibility condition is transformed into 2D constraints which are considered at the element level for the elimination of the stretching parameters. Three-dimensional (3D) energy density is finally replaced by a 2D formulation presenting the starting point of the succeeding finite element formulation.

## 2. GEOMETRY OF THE UNDEFORMED STATE

In this paper, shell theory relations will be presented in tensor notation. Latin indices represent the number 1, 2, 3 and the Greek ones the number 1, 2. For convenience the essential notations to be used in the derivation are firstly summarized in the following:

$X^i$	orthogonal Cartesian coordinates
$\mathbf{i}_j = \mathbf{i}^j$	unit base vectors associated with $X^i$
$\theta^i$	convected curvilinear coordinates of the shell continuum
$(\dots)_x$	partial derivative with respect to the curvilinear coordinates $\theta^x$ of the middle surface $F^{\hat{r}}$
$(\dots),(\dots)$	geometrical elements of the undeformed and deformed state
$\hat{e}_{\alpha\beta}$	permutation tensor associated with $F^{\hat{r}}$
$e^{ijk}, e_{ijk}$	permutation tensor associated with the deformed coordinate $\theta^i, X^i$ .

In this section, the attention is focused to the undeformed shell continuum, the geometrical elements (Fig. 1) of which are to be presented with the suffix  $(\dots)$ . Let  $\hat{\mathbf{r}} = \hat{\mathbf{r}}(\theta^x)$  be the position vector of points  $\hat{P}$  of the middle surface  $F^{\hat{r}}$ , where  $\theta^x$  are curvilinear coordinates. Using  $\hat{\mathbf{r}}$  the geometrical elements of  $F^{\hat{r}}$  can be evaluated by the usual manner. For later use we introduce

$$\text{the base vectors: } \hat{\mathbf{a}}_\alpha = \hat{\mathbf{r}}_{,\alpha}, \quad \hat{\mathbf{a}}^\alpha = \hat{a}^{\alpha\beta} \hat{\mathbf{a}}_\beta, \quad (1)$$

$$\text{the unit normal vector: } \hat{\mathbf{n}}_3 = \hat{\mathbf{a}}_3 = \frac{\hat{\mathbf{a}}_1 \times \hat{\mathbf{a}}_2}{\sqrt{\hat{a}}}, \quad (2)$$

$$\text{the metric tensor: } \hat{a}_{\alpha\beta} = \hat{\mathbf{a}}_\alpha \cdot \hat{\mathbf{a}}_\beta, \quad \hat{a}^{\alpha\beta} = \hat{\mathbf{a}}^\alpha \cdot \hat{\mathbf{a}}^\beta, \quad (3)$$

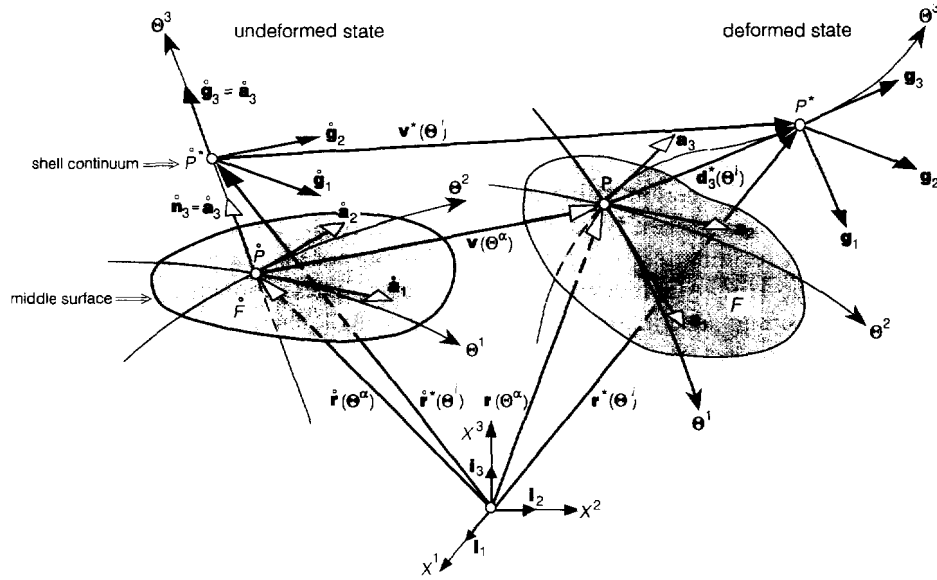


Fig. 1. Deformed and undeformed shell continuum, kinematic variables.

the determinant :  $\hat{a} = |\hat{a}_{\alpha\beta}|$ , (4)

the curvature tensor :  $\hat{b}_{\alpha\beta} = -\hat{a}_{\alpha} \cdot \hat{n}_{3,\beta} = \hat{a}_{\alpha,\beta} \cdot \hat{n}_3$ . (5)

We now consider an arbitrary point  $\hat{P}^*$  of the shell continuum. Let  $\theta^3$  be the distance of  $\hat{P}^*$  from the middle surface  $\hat{F}$ , measured in the  $\hat{n}_3$ -direction. Thus, the position vector  $\hat{r}^*$  of  $\hat{P}^*$  can be represented as

$$\hat{r}^* = \hat{r} + \theta^3 \hat{n}_3, \tag{6}$$

from which following expressions can be derived for the geometrical variables associated with  $\hat{P}^*$ :

the base vectors

$$\hat{g}_\alpha = \hat{a}_\alpha + \theta^3 \hat{n}_{3,\alpha} = \hat{\mu}'_\alpha \hat{a}_\alpha, \quad \hat{g}_3 = \hat{n}_3, \tag{7}$$

$$\hat{\mu}'_\alpha = \delta'_\alpha - \theta^3 \hat{b}'_\alpha, \tag{8}$$

the metric tensor

$$\hat{g}_{\alpha\beta} = \hat{a}_{\alpha\beta} - 2\theta^3 \hat{b}_{\alpha\beta} + (\theta^3)^2 \hat{b}_{\alpha\nu} \hat{b}_{\nu\beta}, \tag{9}$$

$$\hat{g}^{\alpha\beta} = \hat{a}^{\alpha\beta} + 2\theta^3 \hat{b}^{\alpha\beta} + 3(\theta^3)^2 \hat{b}^{\alpha\nu} \hat{b}_{\nu}^{\beta} + \dots, \tag{10}$$

$$\hat{g}_{\alpha 3} = \hat{g}^{\alpha 3} = 0, \quad \hat{g}_{33} = \hat{g}^{33} = 1, \tag{11}$$

the volume element

$$dV^{\hat{}} = \sqrt{\hat{g}} d\theta^1 d\theta^2 d\theta^3, \tag{12}$$

with the determinant

$$\sqrt{\hat{g}} = (\hat{\mathbf{g}}_1 \times \hat{\mathbf{g}}_2) \cdot \hat{\mathbf{g}}_3 = [\hat{\mathbf{g}}_1 \hat{\mathbf{g}}_2 \hat{\mathbf{g}}_3], \tag{13}$$

and finally the determinant of the shifter  $\hat{\mu}_2^{\hat{a}}$

$$\hat{\mu} = \sqrt{\hat{g}/\hat{a}} = |\hat{\mu}_2^{\hat{a}}| = 1 - 2\theta^3 H + (\theta^3)^2 K, \tag{14}$$

with the mean curvature  $H$  and the Gaussian curvature  $K$

$$H = \frac{1}{2} \hat{b}_z^z, \quad K = |\hat{b}_\beta^z|. \tag{15}$$

In the deformed state, geometrical variables will be presented without any mark. Thus, without suffix ( $\hat{\cdot}$ ), the expressions (1–5) and (12, 13) hold for the deformed state. We, however, note that expressions similar to those given in (7–11) and (14) do not hold for the deformed case, since in the present development the position vector  $\mathbf{r}^*$  will be described, as distinct from (6), by a quadratic series expansion.

### 3. DEFORMATION STATE

The aim of a shell theory is the simulation of the deformation behavior of the shell continuum by 2D displacement and strain variables to be introduced in this section. In dealing with large strains emphasis is to be given to an adequate consideration of transverse strains  $\gamma_{33}$ . Particularly, in the case of rubber-like materials, transverse strains  $\gamma_{33}$  play a very important role in the analysis as they are related, due to the incompressibility condition, directly to shear deformations  $\gamma_{23}$  and the tangential strains  $\gamma_{\alpha\beta}$ . Accordingly the main thrust in the large-strain analysis is the uniform approximation of the three groups of deformations  $\gamma_{\alpha\beta}$ ,  $\gamma_{23}$  and  $\gamma_{33}$  in the internal potential energy starting from a suitable kinematic approach of the displacement field.

Let  $\mathbf{r}^* = \mathbf{r}^*(\theta^i)$  be the position vector of an arbitrary point  $P^*$  of the deformed shell continuum. In the present derivation,  $\mathbf{r}^*$  is supposed to be described by a quadratic series expansion in thickness coordinate  $\theta^3$  (Fig. 1):

$$\mathbf{r}^* = \mathbf{r}(\theta^\alpha) + \mathbf{d}_3^*(\theta^i) = \mathbf{r} + \theta^3 \lambda \mathbf{d}_3 + (\theta^3)^2 \mathbf{u} \tag{16}$$

with a director  $\mathbf{d}_3$  constrained by the inextensibility condition

$$\mathbf{d}_3 \cdot \mathbf{d}_3 = 1 \rightarrow \mathbf{d}_{3,\alpha} \cdot \mathbf{d}_3 = 0. \tag{17}$$

Accordingly, the kinematic model (16) involves nine unknown parameters. The multiplicative decomposition of the first-order term in eqn (16) originally suggested by Simo *et al.* (1990b) provides the advantage that the numerically sensitive stretching parameter  $\lambda$  is decoupled from  $\mathbf{d}_3$  subjected in view of eqn (17) to pure rotations. A further advantage is that, for  $\lambda = 1$  and  $\mathbf{u} = 0$ , the kinematic model (16) reduces to that commonly adopted in finite rotation models [Başar *et al.* (1992)] which are therefore involved in the present formulation as a special case.

Our next goal is the definition of 2D strain variables on the basis of the Green's strain tensor

$$\boldsymbol{\gamma} = \gamma_{ij} \hat{\mathbf{g}}^i \otimes \hat{\mathbf{g}}^j = \frac{1}{2} (g_{ij} - \hat{g}_{ij}) \hat{\mathbf{g}}^i \otimes \hat{\mathbf{g}}^j, \tag{18}$$

where the base vectors  $\mathbf{g}_i$  are according to eqn (16) given by

$$\mathbf{g}_x = \mathbf{a}_x + \theta^3 (\lambda_{,x} \mathbf{d}_3 + \lambda \mathbf{d}_{3,x}) + (\theta^3)^2 \mathbf{u}_x, \quad (19)$$

$$\mathbf{g}_3 = \lambda \mathbf{d}_3 + 2\theta^3 \mathbf{u}. \quad (20)$$

Inserting the above results together with eqn (7) in eqn (18) delivers

$$\hat{\gamma}_{ij} = \begin{bmatrix} \hat{\gamma}_{x\beta} & \hat{\gamma}_{x3} \\ \hat{\gamma}_{3x} & \hat{\gamma}_{33} \end{bmatrix} = \begin{bmatrix} \sum_{n=0}^2 (\theta^3)^n \hat{\gamma}_{x\beta}^n & \sum_{m=0}^1 (\theta^3)^m \hat{\gamma}_{x3}^m \\ \sum_{m=0}^1 (\theta^3)^m \hat{\gamma}_{3x}^m & \sum_{m=0}^1 (\theta^3)^m \hat{\gamma}_{33}^m \end{bmatrix}, \quad (21)$$

with 2D strains  $\hat{\gamma}_{x\beta}^n (n = 0, 1, 2)$  and  $\hat{\gamma}_{i3}^m (m = 0, 1)$  subjected to the following constraints: tangential strains

$$\hat{\gamma}_{x\beta}^0 = \frac{1}{2} (\mathbf{a}_x \cdot \mathbf{a}_\beta - \hat{\mathbf{a}}_x \cdot \hat{\mathbf{a}}_\beta), \quad (22)$$

$$\hat{\gamma}_{x\beta}^1 = \frac{1}{2} [\lambda (\mathbf{d}_{3,\beta} \cdot \mathbf{a}_x + \mathbf{d}_{3,x} \cdot \mathbf{a}_\beta) + \lambda_{,x} \mathbf{d}_3 \cdot \mathbf{a}_\beta + \lambda_{,\beta} \mathbf{d}_3 \cdot \mathbf{a}_x - (\hat{\mathbf{a}}_x \cdot \hat{\mathbf{n}}_{3,\beta} + \hat{\mathbf{a}}_\beta \cdot \hat{\mathbf{n}}_{3,x})], \quad (23)$$

$$\hat{\gamma}_{x\beta}^2 = \frac{1}{2} (\mathbf{u}_x \cdot \mathbf{a}_\beta + \mathbf{u}_\beta \cdot \mathbf{a}_x + \lambda_{,x} \lambda_{,\beta} + \lambda^2 \mathbf{d}_{3,x} \cdot \mathbf{d}_{3,\beta} - \hat{\mathbf{n}}_{3,x} \cdot \hat{\mathbf{n}}_{3,\beta}), \quad (24)$$

transverse shear strains

$$\hat{\gamma}_{x3}^0 = \frac{1}{2} \lambda \mathbf{a}_x \cdot \mathbf{d}_3, \quad (25)$$

$$\hat{\gamma}_{x3}^1 = \frac{1}{2} (\lambda \lambda_{,x} + 2\mathbf{u} \cdot \mathbf{a}_x) = \frac{1}{2} (\lambda \lambda_{,x} + 2\bar{u}_x), \quad (26)$$

transverse normal strains

$$\hat{\gamma}_{33}^0 = \frac{1}{2} (\lambda^2 - 1), \quad (27)$$

$$\hat{\gamma}_{33}^1 = 2\lambda \mathbf{d}_3 \cdot \mathbf{u} = 2\lambda \bar{u}_3. \quad (28)$$

In view of the approximation of  $\mathbf{g}_x$  by eqn (19), series expansions for tangential components  $\hat{\gamma}_{x\beta}$  have been broken down in (21) after the quadratic  $\theta^3$ -term while  $\hat{\gamma}_{x3}$  and  $\hat{\gamma}_{33}$  have been, in accordance with eqn (20), approximated by linear expressions in  $\theta^3$ . The notation (..) used for 2D strains  $\hat{\gamma}_{ij}^n$  will be used systematically in the subsequent derivation to indicate coefficients of power series in  $\theta^3$  in the following sense:

$$N = \hat{N}^0 + \theta^3 \hat{N}^1 + (\theta^3)^2 \hat{N}^2 + \dots, \quad \hat{N}^n = \frac{1}{n!} (N_{,33\dots3})|_{\theta^3=0}. \quad (29)$$

By means of (18–20), it can easily be confirmed that the expressions given in (22–28) for 2D strains can be obtained according to the above rule.

The new variable  $\bar{u}_3$  occurring in eqn (28) is defined by the decomposition of the vector  $\mathbf{u}$  with respect to the deformed basis  $(\mathbf{a}_x, \mathbf{d}_3)$  as

$$\mathbf{u} = \bar{u}^\beta \mathbf{a}_\beta + \bar{u}^3 \mathbf{d}_3 = \bar{u}_\beta \mathbf{a}^\beta + \bar{u}_3 \mathbf{d}^3. \quad (30)$$

From eqns (27) and (28) it can easily be seen that  $\bar{u}_3$  describes together with  $\lambda$  through-thickness stretchings completely. On the contrary, the tangential components  $\bar{u}_x$  have no influence on transverse normal strains  $\hat{\gamma}_{33}$ . This demonstrates the mechanical significance of the decomposition (30) with respect to the deformed basis. The decomposition (30) permits furthermore to transform the initial approach (16) into a number of simplified

Table 1. Various theoretical models and their notations

Theoretical model	SD-9	SD-7	SD-6
Kinematic assumption	$\mathbf{r}^* = \mathbf{r} + \theta^3 \lambda \mathbf{d}_3 + (\theta^3)^2 \mathbf{u}$	$\mathbf{r}^* = \mathbf{r} + \theta^3 (\lambda + \theta^3 \bar{u}_3) \mathbf{d}_3$	$\mathbf{r}^* = \mathbf{r} + \theta^3 \lambda \mathbf{d}_3$
Constraints		$\mathbf{d}_3 \cdot \mathbf{d}_3 = 1$ or $\mathbf{d}_3 = \mathbf{d}_3(\psi_x)$	
2D strains		$\gamma_{x\beta} = \sum_n (\theta^3)^n \gamma_{x\beta}^n, \quad \gamma_{33} = \sum_k (\theta^3)^k \gamma_{33}^k$	
	$n = 0, 1, 2; k = 0, 1$	$n = 0, 1, 2; k = 0, 1$	$n = 0, 1; k = 0$
Independent variables	9: $\mathbf{r}, \psi_x, \lambda, \mathbf{u}$ 7: $\mathbf{r}, \psi_x, \bar{u}_3$	for compressible materials 7: $\mathbf{r}, \psi_x, \lambda, \bar{u}_3$ for incompressible materials 5: $\mathbf{r}, \psi_x$	6: $\mathbf{r}, \psi_x, \lambda$ 5: $\mathbf{r}, \psi_x$

models being of significance for numerical applications. If compressible materials are considered then the tangential components  $\bar{u}_x$  can be suppressed without a significant loss of accuracy [Başar and Ding (1994)], but the inclusion of  $\bar{u}_3$  is in this case essential to achieve lock-free models able to consider transverse strains  $\gamma_{33}$ . For incompressible materials  $\bar{u}_3$  is not needed as a remedy against locking and can also be neglected. Thus, the analysis can be carried out in this case by means of the linear expression  $\mathbf{r}^* = \mathbf{r} + \theta^3 \lambda \mathbf{d}_3$  evaluating the stretching parameter  $\lambda$  through the incompressibility condition. For the development of numerical models applicable both to compressible and incompressible materials a kinematic model involving at least a scalar-valued parameter  $\bar{u}_3$  as a quadratic term is however indispensable. Simplified models discussed above are collected in Table 1 where the notations (e.g. SD-9) indicate the number of unknown parameters involved in each individual model.

Concludingly we construct according to eqn (18) the mixed components  $\gamma_i^j$  of the strain tensor. This yields by using eqns (10) and (21) within the present accuracy level

$$\begin{aligned}
 \gamma_x^\beta &= \gamma_{23} \hat{\theta}^{j\beta} = \gamma_x^\beta + \theta^3 (\gamma_x^\beta + 2b_{\rho\gamma}^{\beta 0}) + (\theta^3)^2 (\gamma_x^\beta + 2b_{\rho\gamma}^{\beta 1} + 3b_{\rho\gamma}^{\beta 0} \gamma_x^\rho), \\
 \gamma_x^3 &= \gamma_{23} \hat{\theta}^{j3} = \gamma_{23} = \gamma_{x3}^0 + \theta^3 \gamma_{x3}^1, \\
 \gamma_3^x &= \gamma_{31} \hat{\theta}^{jx} = \gamma_3^x + \theta^3 (\gamma_3^x + 2b_{\rho\gamma}^x \gamma_3^\rho), \\
 \gamma_3^3 &= \gamma_{31} \hat{\theta}^{j3} = \gamma_{33} = \gamma_{33}^0 + \theta^3 \gamma_{33}^1
 \end{aligned} \tag{31}$$

where mixed components of 2D strains are defined with respect to the midsurface basis, e.g. as:

$$\gamma_x^\rho = \gamma_{x\beta} \hat{a}^{\beta\rho}, \quad \gamma_x^{\rho\beta} = \gamma_{\rho\gamma} \hat{a}^{\rho\beta}. \tag{32}$$

#### 4. KINEMATIC RELATIONS

Kinematic relations (22–28) are now to be transformed in component form. As we prefer here the isoparametric finite element formulation, the vectors appearing in eqn (16) will be defined with respect to the fixed orthonormal Cartesian basis  $\mathbf{i}_j$ . By denoting the resulting components by upper case letters we then have

$$\mathbf{r} = X^j \mathbf{i}_j, \quad \mathbf{d}_3 = D^j \mathbf{i}_j, \quad \mathbf{u} = U^j \mathbf{i}_j \tag{33}$$

where the new components  $U^j$  are related to the previous ones  $\bar{u}^j$  by

Table 2. Kinematic relations and incompressibility conditions

Kinematic relations :

$$\begin{aligned} \frac{\partial}{\partial t} X_{\alpha\beta}^1 &= \frac{1}{2} X_{,\alpha}^1 X_{,\beta}^1 - X_{,\alpha}^1 X_{,\beta}^1 \delta_{\alpha\beta} \\ \frac{\partial}{\partial t} X_{\alpha\beta}^1 &= \frac{1}{2} [\lambda(X_{,\alpha}^1 D_{,\beta}^1 + X_{,\beta}^1 D_{,\alpha}^1) + \lambda_{,\alpha} X_{,\beta}^1 D^1 + \lambda_{,\beta} X_{,\alpha}^1 D^1 \\ &\quad - (X_{,\alpha}^1 N_{,\beta}^1 + X_{,\beta}^1 N_{,\alpha}^1)] \delta_{\alpha\beta} \\ \frac{\partial}{\partial t} X_{\alpha\beta}^2 &= \frac{1}{2} [(U_{,\alpha}^1 X_{,\beta}^1 + U_{,\beta}^1 X_{,\alpha}^1 + \lambda^2 D_{,\alpha}^1 D_{,\beta}^1 - N_{,\alpha}^1 N_{,\beta}^1) \delta_{\alpha\beta} + \lambda_{,\alpha} \lambda_{,\beta}] \\ \frac{\partial}{\partial t} X_{\alpha\beta}^3 &= \frac{1}{2} \lambda X_{,\alpha}^1 D_{,\beta}^1 \delta_{\alpha\beta} \\ \frac{\partial}{\partial t} X_{\alpha\beta}^3 &= \frac{1}{2} (\lambda \lambda_{,\alpha} + 2 U^1 X_{,\alpha}^1) \delta_{\alpha\beta} \\ \frac{\partial}{\partial t} X_{\alpha\beta}^3 &= \frac{1}{2} (\lambda^2 - 1) \\ \frac{\partial}{\partial t} X_{\alpha\beta}^3 &= 2 \lambda D^1 U^1 \delta_{\alpha\beta} \end{aligned}$$

Incompressibility conditions :

$$\begin{aligned} \lambda &= \frac{\bar{a}}{X_{,\alpha}^1 X_{,\beta}^1 D^k e_{\alpha\beta k}} \\ \bar{a} &= \frac{1}{2} e^{\alpha\beta} \lambda [X_{,\alpha}^1 X_{,\beta}^1 N^k - \lambda^2 X_{,\alpha}^1 D_{,\beta}^1 D^k] e_{\alpha\beta k} \end{aligned}$$

$$U^j = \mathbf{u} \cdot \mathbf{i}_j = (\bar{u}^\beta \mathbf{a}_\beta + \bar{u}^3 \mathbf{d}_3) \cdot \mathbf{i}_j = X_{,\beta}^1 \bar{u}^\beta + D^3 \bar{u}^3 \tag{34}$$

with  $\mathbf{a}_\beta = \mathbf{r}_{,\beta}$  and  $\mathbf{d}_3$  being the base vectors of the deformed midsurface. Inserting now eqn (33) as well as the expressions  $\hat{\mathbf{r}} = X^j \mathbf{i}_j$ ,  $\hat{\mathbf{d}}_3 = \hat{\mathbf{n}}_3 = N^j \mathbf{i}_j$  into (22–28), we easily obtain the kinematic relations summarized in Table 2 where  $\delta_{\alpha\beta}$  is the well-known Kronecker symbol.

The inextensibility condition (17) being a nonlinear relation in terms of the unknown variable  $\mathbf{d}_3$  causes necessarily numerical difficulties if large rotations are involved in the analysis. To ensure *a priori* satisfaction of the constraint (17) and thus to avoid its explicit consideration a number of efficient procedures such as Euler angles [Ramm (1976) ; Başar *et al.* (1993)], updated formulation [Simo *et al.* (1990b)] etc. are available in literature. Here we prefer to use Euler angles  $\psi_x$  (Fig. 2) determining the director  $\mathbf{d}_3$  with respect to the fixed basis  $\mathbf{i}_j$  as

$$D^1 = \sin \psi_1 \cos \psi_2, \quad D^2 = \sin \psi_1 \sin \psi_2, \quad D^3 = \cos \psi_1. \tag{35}$$

In the FE-procedure  $\psi_x$  will be used as primary variables. The shape functions of the director  $D^j$  are then to be constructed by means of the above constraints (35) implying the inextensibility condition  $\mathbf{d}_3 \cdot \mathbf{d}_3 = 1$ . In this context we note that updated formulation with a three parametric rotation vector becomes more advantageous than the above procedure if shells with geometry intersections are considered. This aspect will be however treated in a further work.

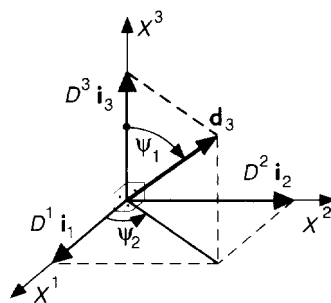


Fig. 2. Definition of the rotation variables  $\psi_x$ .

5. STRAIN INVARIANTS AND INCOMPRESSIBILITY CONDITIONS

All equations presented above are valid for arbitrary materials. We now confine our attention to rubber components characterized by incompressibility, that is, preservation of volume during deformation. The related deformations are called isochoric. Thus we shall introduce in this section first the strain invariants  $I_1, I_2$  needed for the formulation of the corresponding strain energy density. The next goal will be the transformation of the incompressibility condition  $I_3 = 1$  into 2D constraints compatible with the kinematic approach (16). This set of equations is needed for the elimination of the stretching parameters  $\lambda$  and  $\bar{u}_3$  presenting in this case dependent quantities.

By means of the abbreviations

$$\begin{aligned}
 A &= 2\gamma_x^2, & D &= \frac{1}{2}(\gamma_x^2\gamma_\beta^\beta - \gamma_\beta^2\gamma_x^\beta), & N &= A + 4D, & Q &= \gamma_x^3\gamma_3^3, \\
 S &= -4[\gamma_3^x\gamma_x^3 - 2\gamma_3^2(\gamma_{\beta 3}\gamma_x^\beta - \gamma_{x 3}\gamma_\beta^\beta)], & R &= \frac{S + N}{1 + N}
 \end{aligned}
 \tag{36}$$

to be used systematically in subsequent derivations the first two strain invariants  $I_1$  and  $I_2$  are given by

$$I_1 = 3 + A + 2\gamma_3^3, \quad I_2 = 3 + 2A + 4D + 2\gamma_3^3(2 + A) - 4Q.
 \tag{37}$$

Similarly, the incompressibility condition  $I_3 = 1$  can be transformed into the form

$$\gamma_{33} = -\frac{1}{2}R = -\frac{1}{2}\frac{S + N}{1 + N}
 \tag{38}$$

which will be used for the elimination of  $\gamma_{33}$  in the strain energy density (43). We note that, in eqn (36),  $S$  vanishes for  $\gamma_{x3} = 0$  while the definitions (36) for  $A, D, N$  and  $R$  preserve also in this case their validity.

In view of (13) equation  $I_3 = 1$  may also be replaced equivalently by the relation

$$\sqrt{g} = (\mathbf{g}_1 \times \mathbf{g}_2) \cdot \mathbf{g}_3 = \sqrt{\hat{g}} = (\hat{\mathbf{g}}_1 \times \hat{\mathbf{g}}_2) \cdot \hat{\mathbf{g}}_3.
 \tag{39}$$

To transform (39) into 2D conditions we express the base vectors  $\mathbf{g}_i$  and  $\hat{\mathbf{g}}_i$  according to eqns (19), (20) and (7). Then we equate in the resulting series expansion in  $\theta^3$  the first two coefficients to zero. By considering eqn (30) this procedure leads to the following two constraints.

$$\lambda = \frac{[\hat{\mathbf{a}}_1 \hat{\mathbf{a}}_2 \hat{\mathbf{n}}_3]}{[\mathbf{a}_1 \mathbf{a}_2 \mathbf{d}_3]} = \frac{\sqrt{\hat{a}}}{[\mathbf{a}_1 \mathbf{a}_2 \mathbf{d}_3]},
 \tag{40}$$

$$\bar{u}_3 = \frac{1}{2}\hat{\epsilon}^{2\beta}\lambda[(\hat{\mathbf{a}}_x \times \hat{\mathbf{n}}_{3,\beta}) \cdot \hat{\mathbf{n}}_3 - \lambda^2(\mathbf{a}_x \times \mathbf{d}_{3,\beta}) \cdot \mathbf{d}_3],
 \tag{41}$$

which will be used at the element level for the elimination of the stretching parameter  $\lambda$  and  $\bar{u}_3$ . The above result (41) emphasizes the suitability of the decomposition (30) which permits the evaluation of  $\bar{u}_3$  independently of the tangential components  $\bar{u}_x$ . Both relations (40) and (41) have been transformed by using eqn (33) in component relations given in Table 2.

6. INTERNAL POTENTIAL ENERGY

In this section attention is again focused to rubber-like materials with the aim to derive for the internal potential energy a consistent 2D expression. Thus the later FE-implementation can be carried out by means of a formulation the consistency of which as 2D approximation is ensured. This will lead to a so-called shell theory FE-model.

Let  $\pi_i^* = \pi_i^*(\gamma_{ij})$  denote the strain energy per unit volume of the undeformed state. For a shell of thickness  $h$  the internal potential energy is then given by

$$\Pi_i = \iiint_V \pi_i^* dV^0 = \iint_{F^0} \pi_i dF^0 \rightarrow \pi_i = \int_{-h/2}^{h/2} \hat{\mu} \pi_i^* d\theta^3 \quad (42)$$

with the midsurface element  $dF^0 = \sqrt{\hat{a}} d\theta^1 d\theta^2$  and the scalar-valued function  $\hat{\mu} = \sqrt{\hat{g}/\hat{a}}$ , which can be approximated, as usual in shell theory formulations, by  $\hat{\mu} \approx 1$ . In eqn (42),  $\pi_i$  denotes strain energy per unit area of midsurface  $F^0$ . Like arbitrary hyperelastic materials, rubber-like components can be modeled through the strain energy density  $\pi_i^*$ . The most popular model for incompressible materials is the well-known Mooney–Rivlin model given in terms of the strain invariants  $I_1$  and  $I_2$  by

$$\pi_i^* = c_1(I_1 - 3) + c_2(I_2 - 3) \quad (43)$$

with two material constants  $c_1$  and  $c_2$ . For  $c_1 = c$  and  $c_2 = 0$  this model reduces to

$$\pi_i^* = c(I_1 - 3) \quad (44)$$

describing the so-called neo-Hookean materials. As further important incompressible models we also note the Ogden-model

$$\pi_i^* = \pi_i^*(\lambda_1, \lambda_2, \lambda_3) = \sum_{n=1}^3 \frac{\mu_n}{\alpha_n} [(\lambda_1)^{\alpha_n} + (\lambda_2)^{\alpha_n} + (\lambda_3)^{\alpha_n} - 3] \quad (45)$$

representing a function of principal stretches  $\lambda_i$  with  $\mu_n$  and  $\alpha_n$  as material constants and the model due to Hart-Smith and Crisp (1967).

$$\frac{\partial \pi_i^*}{\partial I_1} = G \exp k_1(I_1 - 3)^2, \quad \frac{\partial \pi_i^*}{\partial I_2} = G \frac{k_2}{I_2}, \quad (46)$$

where  $\pi_i^*$  is simulated in an exponential hyperbolic form,  $G$ ,  $k_1$  and  $k_2$  being the related material constants. The Ogden model (45) requires the transformation of actual strains  $\gamma_{ij}$  in principal stretches and may be therefore in bending analysis computationally rather expensive. The model has been used mainly in membrane shell elements [Wriggers and Taylor (1990); Gruttmann and Taylor (1992)]. In the present FE-implementation the first two models (43) and (44) will be considered.

To explain the derivation of 2D strain energy function we refer to the Mooney–Rivlin model (43), where we replace  $I_1$  and  $I_2$  by eqn (37) in order to eliminate  $\gamma_{33}$  by considering eqn (38). This leads to

$$\pi_i^* = c_1(A - R) + c_2[2A + 4D - (2 + A)R - 4Q] \quad (47)$$

with the abbreviations  $A, D, \dots$  given in eqn (36). We now expand  $\pi_i^*$  (47), according to eqn (29), into a power series in  $\theta^3$  which we then introduce into eqn (42). Since all odd terms in  $\theta^3$  vanish after thickness integration, we obtain as final result within the present accuracy level

$$\Pi_i = \iint_{F^0} \left[ h\pi_i^0 + \frac{h^3}{12}\pi_i^2 + \frac{h^5}{80}\pi_i^4 \right] dF^0, \quad (48)$$

where the relevant coefficients  $\pi_i^0$ ,  $\pi_i^2$  and  $\pi_i^4$  are given by

$$\overset{0}{\pi}_i = c_1(\overset{0}{A} - \overset{0}{R}) + c_2[2\overset{0}{A} + 4\overset{0}{D} - (2 + \overset{0}{A})\overset{0}{R} - 4\overset{0}{Q}], \quad (49)$$

$$\overset{2}{\pi}_i = c_1(\overset{2}{A} - \overset{2}{R}) + c_2[(2 - \overset{0}{R})\overset{2}{A} + 4\overset{2}{D} - (2 + \overset{0}{A})\overset{2}{R} - \overset{1}{A}\overset{1}{R} - 4\overset{2}{Q}], \quad (50)$$

$$\overset{4}{\pi}_i = -c_1\overset{4}{R} + c_2[4\overset{4}{D} - (2 + \overset{0}{A})\overset{4}{R} - \overset{1}{A}\overset{3}{R} - \overset{2}{A}\overset{2}{R}], \quad (51)$$

The abbreviations  $\overset{0}{A}, \overset{0}{D}, \dots$ , involved in the above relations can be, by considering eqns (21) and (29), evaluated from eqn (36). As examples, expressions for these variables up to the second-order are given in Appendix 1.

As starting point of the FE-implementation the principle of virtual work  $\delta^*A = \delta^*A_a + \delta^*A_i = 0$  is finally to be introduced which can easily be constructed by means of the equality  $\delta^*A_i = -\delta\Pi_i$  characterizing any hyperelastic material. We denote surface loads per unit area of the undeformed midsurface  $F^0$  by  $\mathbf{p}$  and line loads per unit of the undeformed boundary  $C^0$  by  $\mathbf{n}^0$ . Both load actions are supposed to be conservative. Thus the principle of virtual work is described by

$$\delta^*A = \delta^*A_a + \delta^*A_i = \iint_{F^0} \mathbf{p}^0 \cdot \delta\mathbf{v} \, dF^0 + \int_{C^0} \mathbf{n}^0 \cdot \delta\mathbf{v} \, ds - \iint_F \left( h \delta\pi_i^0 + \frac{h^3}{12} \delta\pi_i^2 + \frac{h^5}{80} \delta\pi_i^4 \right) dF^0. \quad (52)$$

With a slight modification of the first integral ( $\mathbf{p}^0 \rightarrow \sqrt{a/\hat{a}} \mathbf{p}$ ) the above relation can be used also for deformation dependent loads  $\mathbf{p}$  referring to the unit area of the deformed state  $F$ . If attention is further restricted to pressure due to fluids then we have  $\mathbf{p} = \pm q \mathbf{n}_3$  with  $\mathbf{n}_3$  as the unit normal of  $F$  and  $q$  the load intensity (per unit area  $F$ ).

### 7. CONSTITUTIVE RELATIONS

Once the displacement variables and, by means of eqn (21), 3D strains  $\gamma_{ij}$  are computed in the FE-procedure, through-thickness distributions of the stress can be evaluated from the constitutive relations to be established in this section. For this purpose, we again distinguish between two cases. If the shell material is compressible, the Cauchy stress tensor  $\tau^{ij}$  is given by [Green and Zerna (1968)]

$$\tau^{ij} = \Phi \hat{g}^{ij} + \Psi B^{ij} + P g^{ij}, \quad (53)$$

where the scalar valued functions

$$\Phi = \frac{2}{\sqrt{I_3}} \frac{\partial \pi_1^*}{\partial I_1}, \quad \Psi = \frac{2}{\sqrt{I_3}} \frac{\partial \pi_1^*}{\partial I_2}, \quad P = 2\sqrt{I_3} \frac{\partial \pi_1^*}{\partial I_3} \quad (54)$$

are closely connected with the strain energy density  $\pi_1^*$ , in the present case with eqn (43) or (44), and

$$B^{ij} = I_1 \hat{g}^{ij} - \hat{g}^{ir} \hat{g}^{js} g_{rs} \quad (55)$$

is a tensorial quality depending on  $\gamma_{ij}$  through  $I_3$  and  $g_{rs}$ . In view of the definitions (10, 11), relation (53) takes the form

$$\tau^{\alpha\beta} = \Phi \hat{g}^{\alpha\beta} + \Psi B^{\alpha\beta} + P g^{\alpha\beta}, \quad \tau^{\alpha 3} = \Psi B^{\alpha 3} + P g^{\alpha 3}, \quad \tau^{33} = \Phi + \Psi B^{33} + P g^{33}. \quad (56)$$

Our next goal is the evaluation of the variables  $g_{ij}$ ,  $g^{ij}$  and  $B^{ij}$  occurring in eqn (56) in terms of the 3D strains  $\gamma_{ij}$ . In view of eqn (18),  $g_{ij}$  is given by  $g_{ij} = \hat{g}_{ij} + 2\gamma_{ij}$ , with which the contravariant components  $g^{ij}$  can be constructed by means of the identity  $g_{ir} g^{rj} = \delta_i^j$ . Alternatively,  $g^{ij}$  may be calculated from the relations

$$\begin{aligned}
 g^{z\beta} &= \frac{1}{I_3} \hat{\mu}^{-2} \hat{\varepsilon}^{\alpha\mu} \hat{\varepsilon}^{\beta\lambda} (g_{\rho\lambda} g_{33} - g_{\rho 3} g_{\lambda 3}), \\
 g^{z3} &= \frac{1}{I_3} \hat{\mu}^{-2} \hat{\varepsilon}^{\alpha\beta} \hat{\varepsilon}^{\rho\nu} g_{\beta\rho} g_{3\nu}, \\
 g^{33} &= \frac{1}{2I_3} \hat{\mu}^{-2} \hat{\varepsilon}^{\alpha\beta} \hat{\varepsilon}^{\rho\nu} g_{\alpha\rho} g_{\beta\nu}
 \end{aligned} \tag{57}$$

obtained on the basis of the identity

$$g^{ri} = \frac{1}{2} \varepsilon^{rst} \varepsilon^{ijk} g_{sj} g_{tk} \tag{58}$$

and the definition (14). From eqns (21), (37) and (55) we finally obtain for  $B^{ij}$

$$B^{z\beta} = 2(1 + \gamma_\rho^\rho + \gamma_3^3) \hat{g}^{z\beta} - 2\gamma_i^{z\beta}, \quad B^{z3} = -2\gamma_3^z, \quad B^{33} = 2(1 + \gamma_\rho^\rho). \tag{59}$$

Relations established above for the evaluation of stresses can be easily adopted for incompressible materials by setting  $I_3 = 1$ . An essential distinction is, however, the fact that in the case of incompressible materials the function  $P$  in eqn (54) becomes an unknown variable as the value of the derivative  $\partial \pi^*/\partial I_3$  is not determined at  $I_3 = 1$ . For thin shell structures, the transverse stresses  $\tau^{33}$  in  $\mathbf{d}_3$ -direction are much smaller than other stress components so that they can be neglected without loss of accuracy. In this case  $P$  can be pointwise determined by means of the condition  $\tau^{33} = 0$  and then used for the calculation of other stresses.

### 8. INCREMENTAL FORMULATION

For the development of nonlinear element matrices via an incremental-iterative solution strategy strongly nonlinear shell equations are to be transformed into an incremental formulation. This is accomplished in the present development by a variational procedure. As a detailed description of this procedure can be found in earlier works [e.g. Başar and Ding (1990)], we note here as essential result the incremental formulation of the principle of virtual work. According to eqn (52) it is given by

$$\begin{aligned}
 &\iint_F \frac{h}{2} \left( \bar{\delta} \overset{++}{\pi}_i + \frac{h^2}{12} \bar{\delta} \overset{+-}{\pi}_i + \frac{h^4}{80} \bar{\delta} \overset{+}{\pi}_i \right) dF^\circ \rightarrow \mathbf{k}_i \\
 &= \iint_F \mathbf{p} \cdot \bar{\delta} \overset{+}{\mathbf{v}} dF^\circ + \int \mathbf{n} \cdot \bar{\delta} \overset{+}{\mathbf{v}} ds^\circ \rightarrow \mathbf{p}_e \\
 &- \iint_F h \left( \bar{\delta} \overset{+}{\pi}_i + \frac{h^2}{12} \bar{\delta} \overset{-}{\pi}_i + \frac{h^4}{80} \bar{\delta} \overset{+}{\pi}_i \right) dF^\circ \rightarrow \mathbf{p}_i
 \end{aligned} \tag{60}$$

where  $\bar{\delta}$  implies a variation with respect to the variations  $\delta \mathbf{V} = \overset{+}{\mathbf{V}}$  of the independent displacements  $\mathbf{V}$  and the notation  $(\cdot, \overset{+}{\cdot}) = \delta(\dots)$  and  $(\cdot, \overset{+-}{\cdot}) = \delta^2(\dots)$  denote, respectively, the first- and second-order variational terms, which can be constructed by the usual variational approach. For instance we receive from eqn (49).

$$\overset{+-}{\pi}_i = c_1 (\overset{++}{A} - \overset{++}{R}) + c_2 [(2 - \overset{0}{R}) \overset{+-}{A} + 4 \overset{+-}{D} - (2 + \overset{0}{A}) \overset{++}{R} - 4 \overset{++}{Q} - 2 \overset{++}{A} \overset{++}{R}]. \tag{61}$$

Appendix 2 involves the other relevant results entering in eqn (60). Here it is noticed that the variations  $\overset{+}{X}_i$ ,  $\overset{+}{\psi}_x$  and  $\overset{+}{u}_x$  present primary variables to be approximated independently in the FE-procedure.

To give a further example for the construction of variational equations we refer to the first incompressibility conditions from Table 2 leading to

$$(X^i_{,1} X^j_{,2} D^k e_{ijk})^\dagger = -\lambda (X^i_{,1} X^j_{,2} \bar{D}^k + X^i_{,1} \bar{X}^j_{,2} D^k + \bar{X}^i_{,1} X^j_{,2} D^k) e_{ijk} \tag{62}$$

which will be used in the FE-procedure for the evaluation of the shape function of  $\lambda$ .

The linearization of the tangential stiffness matrix  $\mathbf{k}_t$  can be carried out simply by replacing the geometrical variables of the fundamental state occurring in corresponding relations with those of the undeformed state. For Mooney–Rivlin materials, it has been proved that the stiffness matrix obtained by this linearization process corresponds exactly to that of the classical shell theories [Başar and Krätzig (1985)]

$$\begin{aligned} \mathbf{K}_c &= \iint_{\bar{F}} \left( h \overset{++}{\pi}_i + \frac{h^3}{12} \overset{++}{\pi}_i \right) d\bar{F} \\ &= \iint_{\bar{F}} \left( \frac{Eh}{1-\nu^2} H^{\alpha\beta\rho\zeta} \overset{+}{\gamma} \overset{+}{\alpha\beta\zeta} \overset{+}{\rho\zeta} + 4Gh \overset{+}{\alpha} \overset{+}{\beta} \overset{+}{\gamma} \overset{+}{\delta} \overset{+}{\alpha\beta\gamma\delta} \right) d\bar{F} \\ &\quad + \iint_{\bar{F}} \frac{Eh^3}{12(1-\nu^2)} H^{\alpha\beta\rho\zeta} \overset{+}{\gamma} \overset{+}{\alpha\beta\zeta} \overset{+}{\rho\zeta} d\bar{F} \end{aligned} \tag{63}$$

with

$$H^{\alpha\beta\rho\zeta} = \frac{1-\nu}{2} \left( \overset{+}{\alpha} \overset{+}{\beta} \overset{+}{\gamma} \overset{+}{\delta} + \overset{+}{\alpha} \overset{+}{\beta} \overset{+}{\gamma} \overset{+}{\delta} + \frac{2\nu}{1-\nu} \overset{+}{\alpha} \overset{+}{\beta} \overset{+}{\gamma} \overset{+}{\delta} \right), \tag{64}$$

if Poisson’s ratio  $\nu$  and Young’s modulus  $E$  are selected as  $\nu = 0.5$  and  $E = 6 (c_1 + c_2)$ .

In concluding this section it is worthy to remark that the kinematic model presented in Section 3 can be combined with an arbitrary strain energy function represented in eqn (60) by the second variation of the internal potential energy  $\bar{\pi}_i$ . The Mooney–Rivlin model (43) used in this paper serves only as an example to demonstrate how such a coupling between shell kinematics and material models can be achieved.

### 9. FINITE ELEMENT FORMULATION

The incremental formulation is transformed into a 4-node finite element according to the isoparametric formulation. This model corresponds essentially to a displacement-based model apart the independent approximations of constant shear strains  $\overset{0}{\gamma}_{x3}$ . Here, we shall not deal with the standard FE-procedure, but solely summarize the relevant aspects of the derivation.

Primary displacement quantities  $\bar{X}^i$ ,  $\bar{\psi}_x$  and  $\bar{u}_3$  are interpolated by means of standard bilinear polynomials. We emphasize that the director  $\mathbf{d}_3(\bar{\mathbf{d}}_3, \bar{\mathbf{d}}_3)$  is, in contrast to many formulations [see Büchter *et al.* (1994)], not directly interpolated. Instead, Euler parameters  $\bar{\psi}_x$  are used as primary quantities and the related constraints (35) are considered, as variational equations, to construct the shape functions of  $\bar{\mathbf{d}}_3$  and  $\bar{\mathbf{d}}_3$ . This provides a uniform approximation of the inextensibility condition (17) over the element area.

To avoid shear locking, constant shear deformations are interpolated according to assumed strain concept originally proposed by Dvorkin and Bathe (1984) and described in detail in earlier works [Başar *et al.* (1993); Başar and Ding (1995a)]. It is noted that the first-order terms  $\overset{1}{\gamma}_{x3}$  need not a special treatment in this sense as are numerically stable. Dependent stretching parameters  $\lambda$  and  $\bar{u}_3$  are eliminated at the element level by means of incompressibility conditions.

The element proposed for rubber-components is based on the linear kinematic approach ( $\mathbf{u} = 0$ ) which provides sufficiently accurate results in the case of incompressible structures without locking effects. It is however intended to extend this model to multilayer model (layerwise model) which has been proved from earlier studies to be decisively more predictive than single layer models on the basis of a higher-order displacement

approximation when dealing with e.g. structures involving strongly dissimilar material layers.

The second-order kinematic model of Section 3 has been transformed in an earlier formulation [Başar and Ding (1995)] into a similar finite element model for the analysis of a compressible multilayered shell made of composite materials. The examples presented there demonstrate that this model provides the consideration of both compressible and incompressible shells within a refined approach.

10. NUMERICAL EXAMPLES

Extended numerical studies have been carried out to test the performance of the numerical model proposed with respect to large strain analysis. Some examples have been also analysed by classical finite-rotation elements on the basis of Hookean material for comparison. For this purpose, the Poisson's ratio  $\nu$  and Lamé's constant  $G$  have been selected as  $\nu = 0.5$  and  $G = 2(c_1 + c_2)$  for incompressible materials. The performance of the present model will be now discussed on following examples. All these examples have been analysed using the finite element based on the theoretical model SD-6 in Table 1.

10.1. Uniform extension of a cylindrical tube

We consider a circular cylindrical tube subjected to uniform extension in the longitudinal direction (Fig. 3). If the extension ratio  $\lambda_2$  in this direction is given as the load condition, the extension ratios in other two direction can be obtained by means of the incompressibility condition as

$$\lambda_1 = \frac{R}{r} = \lambda_3 = \frac{H}{h} = \sqrt{1/\lambda_2}$$

and the numerical results for the stresses  $\tau^{(22)}$  in the longitudinal direction can be checked by the analytical solution available in Green and Zerna (1968).

$$\tau^{(22)} = [(\lambda_2)^2 - 1/\lambda_2](2c_1 + 2c_2/\lambda_2).$$

Note that  $\tau^{(ij)}$  are physical components of the Cauchy stress tensor  $\tau^{ij}$ . The analysis has been performed for a 2 shell segment using a single element and considering both material

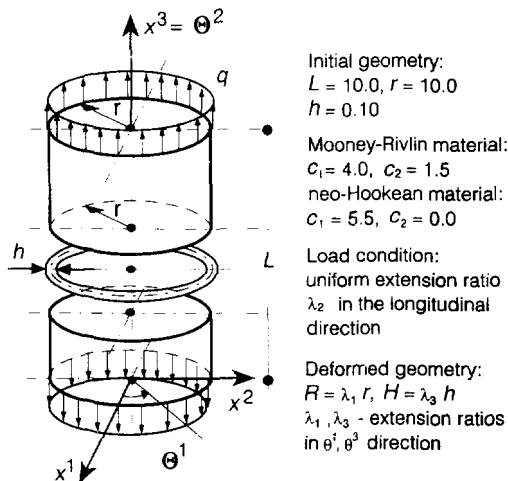


Fig. 3. Uniform extensions of a circular cylindrical tube.

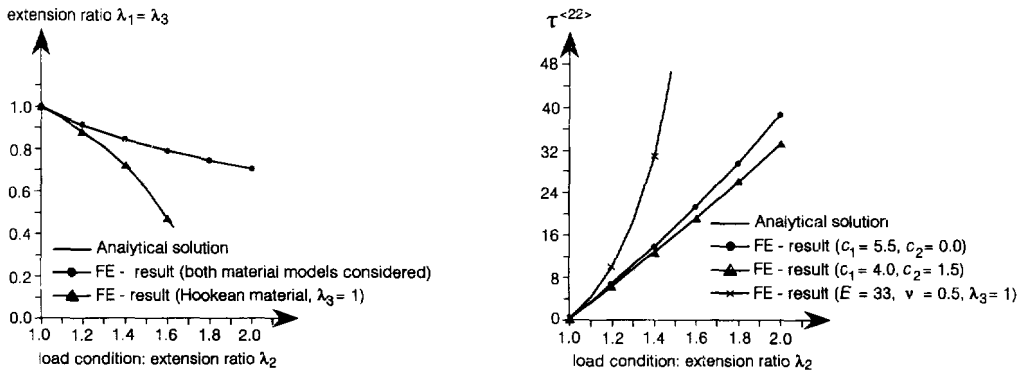


Fig. 4. Uniform extension of a cylindrical tube : load-response diagrams.

models given in Fig. 3. Numerical results shown in Fig. 4 are in full agreement with the analytical solution and thus demonstrate the reliability of the algorithms proposed particularly for the stress calculation. It can be observed that stresses  $\tau^{(22)}$  are, in contrast to the extension ratios  $\lambda_2 = \lambda_3$ , influenced by the material models. Numerical results obtained with the classical Hookean material are also plotted in Fig. 4 for comparison showing clearly that the classical Hookean models [Başar *et al.* (1993)] are not applicable to large strain analysis.

Some other simple examples with existing solutions in literature, such as the simple extension or simple shear of a solid, inflation of a cylindrical tube or a spherical membrane under internal pressure etc., have also been analysed to check the reliability of the numerical model proposed. Numerical results obtained for these simple problems were in excellent agreement with the exact solutions.

10.2. *Stretching of a square sheet with a circular hole*

This problem has been analysed by several authors [see Ramm (1976) ; Parisch (1986) ; Gruttmann and Taylor (1992)]. Due to the symmetry of the structure only one quarter of the sheet is analysed by 64 four-node isoparametric elements (Fig. 5). Our numerical results for the displacements plotted in Fig. 6 show excellent agreement with those of Ramm (1976). The deformed configuration for the load factor  $f = 1.0$  obtained in one loading step and five iterations is given in Fig. 5 demonstrating clearly the large strains involved in the present problem. Numerical results for the thickness stretching parameter  $\lambda$  are presented in Fig. 6. It is interesting to note that the sheet thickness near the point *B* is not decreased but slightly increased during the deformation process. This result suggests the existence of compression stresses near the point *B*. In Fig. 7, the distributions of the thickness stretching

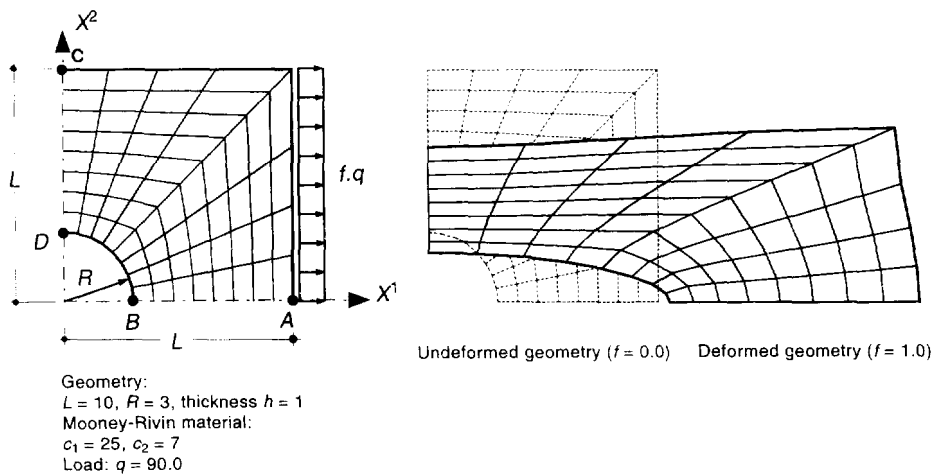


Fig. 5. Stretching of a square sheet with a circular hole : geometry and deformed configuration.

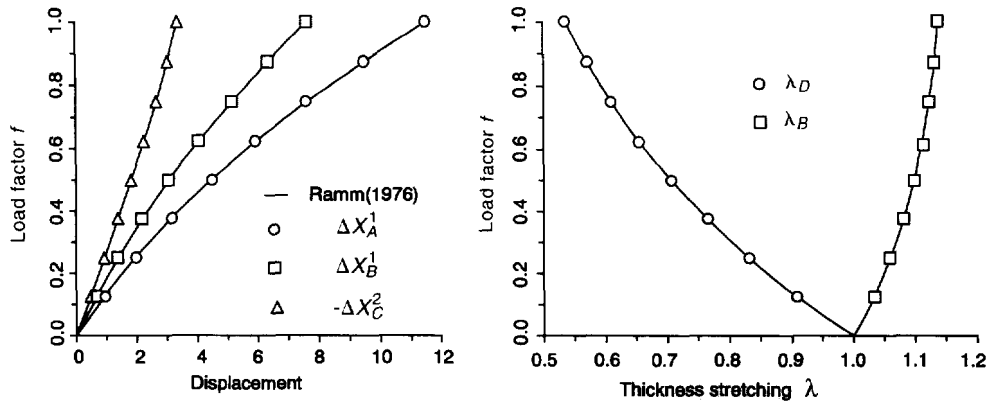
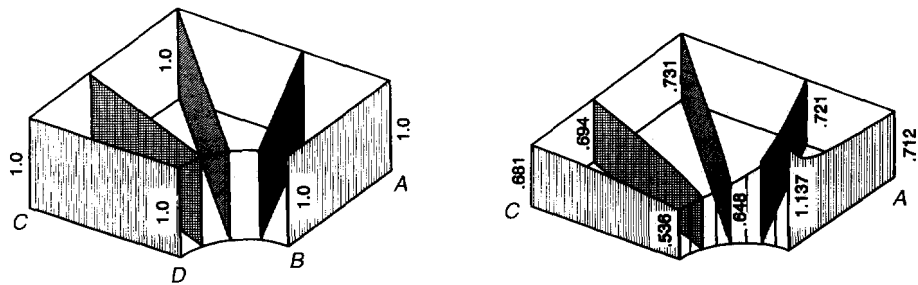


Fig. 6. Stretching of a square sheet : load-deformation diagrams.



Undeformed state ( $f = 0.0$ ):  
 $\lambda = 1.0$  at all points

Thickness stretching  $\lambda$  at  
 the deformed state ( $f = 1.0$ )

Fig. 7. Sheet with a circular hole : distributions of the thickness stretching parameter  $\lambda$ .

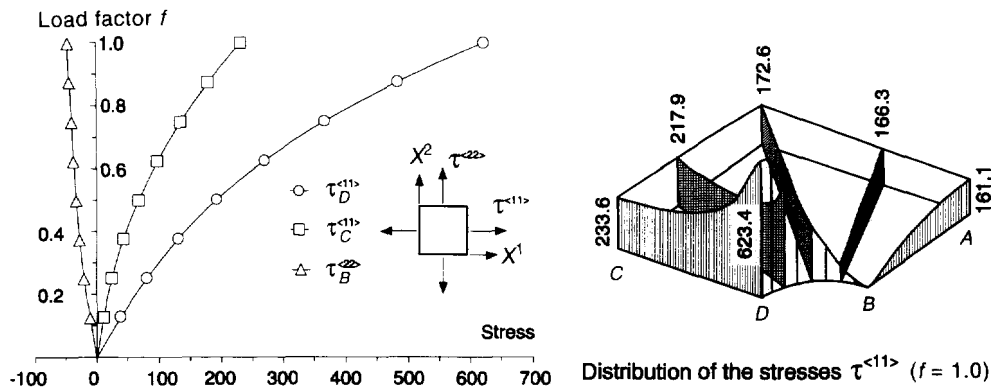


Fig. 8. A square sheet with a circular hole : load-stress diagrams and the stress distribution.

parameter  $\lambda$  are plotted to demonstrate this unusual effect. For an easy physical interpretation, the stresses evaluated originally with respect to convective coordinates are transformed into those referring to the global Cartesian coordinates ( $\tau^{<11>}, \tau^{<22>}$ ). The corresponding results plotted in Fig. 8 confirm the existence of compression stress  $\tau^{<22>}$  near the point  $B$ . We note that the stresses  $\tau^{<11>}$  satisfy zero stress boundary condition at the point  $B$ . To test the accuracy of stress results the stress resultant vectors of the deformed boundary surface  $X^1 = 0$  and  $X^1 = L$  have been evaluated and compared with the acting load resultant. This comparison has demonstrated the numerical error to be almost negligible ( $<0.5\%$ ).

10.3. Hyperbolic shell subjected to nearly concentrated loads

A hyperbolic shell made of hyperelastic material is subjected to four pairs of locally distributed vertical loads (Fig. 9). The deformation of this shell structure is characterized

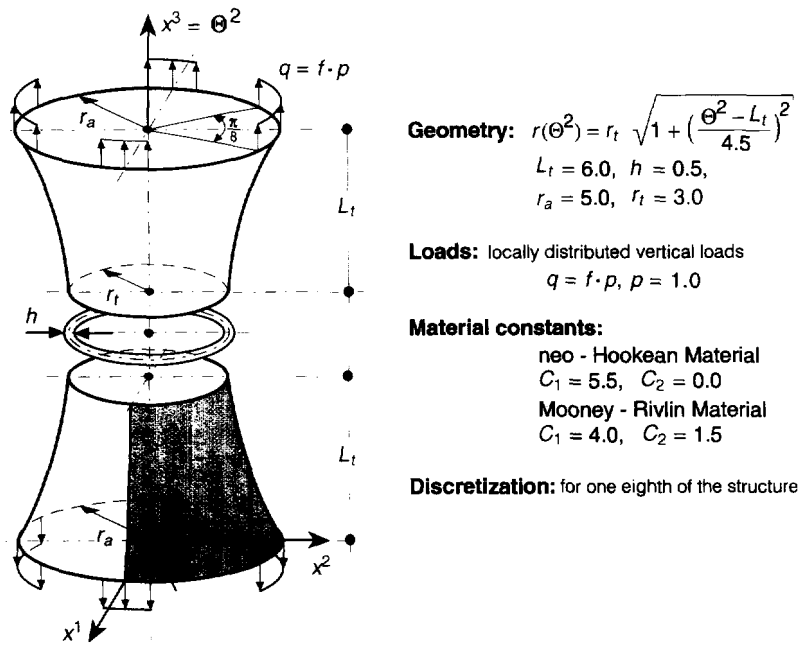


Fig. 9. Hyperboloidal shell under four pairs of locally distributed vertical loads.

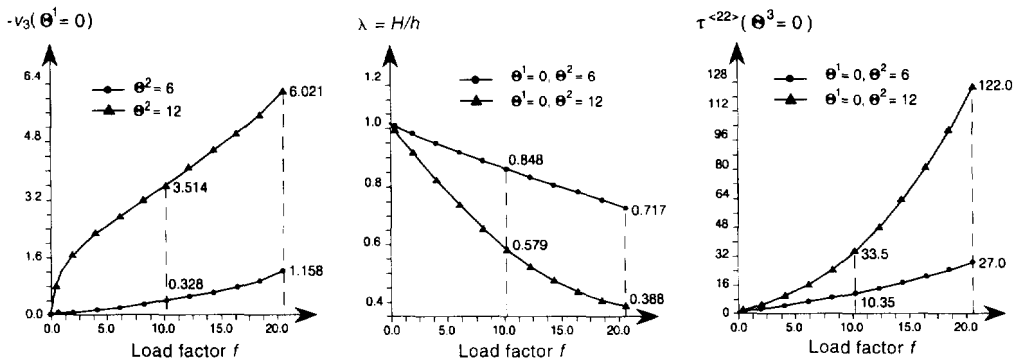


Fig. 10. Hyperboloidal shell: load-response diagrams.

by a combined membrane and bending deformations. Due to the symmetry of the structure and loads, only one eighth of the shell is discretized by  $24 \times 24$  four-node isoparametric elements. Some characteristic results are given in Fig. 10 in the form of load-response diagrams and compared with those obtained with a Kirchhoff–Love type model [Başar and Ding (1996)]. Due to relatively large shell thickness results obtained for the displacement  $\Delta X^3$  show significant discrepancies for large load levels. On the contrary, the stretching parameter  $\lambda$  as well as the middle surface stresses  $\tau^{<22>}$  are practically not affected by the inclusion of shear deformations. Compared with the Kirchhoff–Love model, the present shear-deformation model is computationally more efficient due to the low-order interpolation polynomials used. The undeformed and deformed configurations given in Fig. 12 demonstrate clearly the large displacements and rotations involved in this example. Distributions of the Cauchy stresses  $\tau^{<22>}(\theta^3 = 0)$  and the thickness stretching parameter  $\lambda$  at the load level  $f = 10.0$  and  $f = 20.0$  are plotted in Fig. 11 for some essential sections. For the part of the structure far away from the locally distributed loads, the stress  $\tau^{<22>}(\theta^3 = 0)$  and the thickness stretching  $\lambda$  possess a nearly uniform distribution along the circumferential direction. On the contrary, stress concentrations due to the locally distributed loads can be observed clearly at the section  $\theta^2 = 0$  while the zero stress boundary condition is approximately satisfied along the unloaded parts of the boundaries. The distributions of the thickness stretching given in Fig. 11 show great changes of the shell thickness near the loads

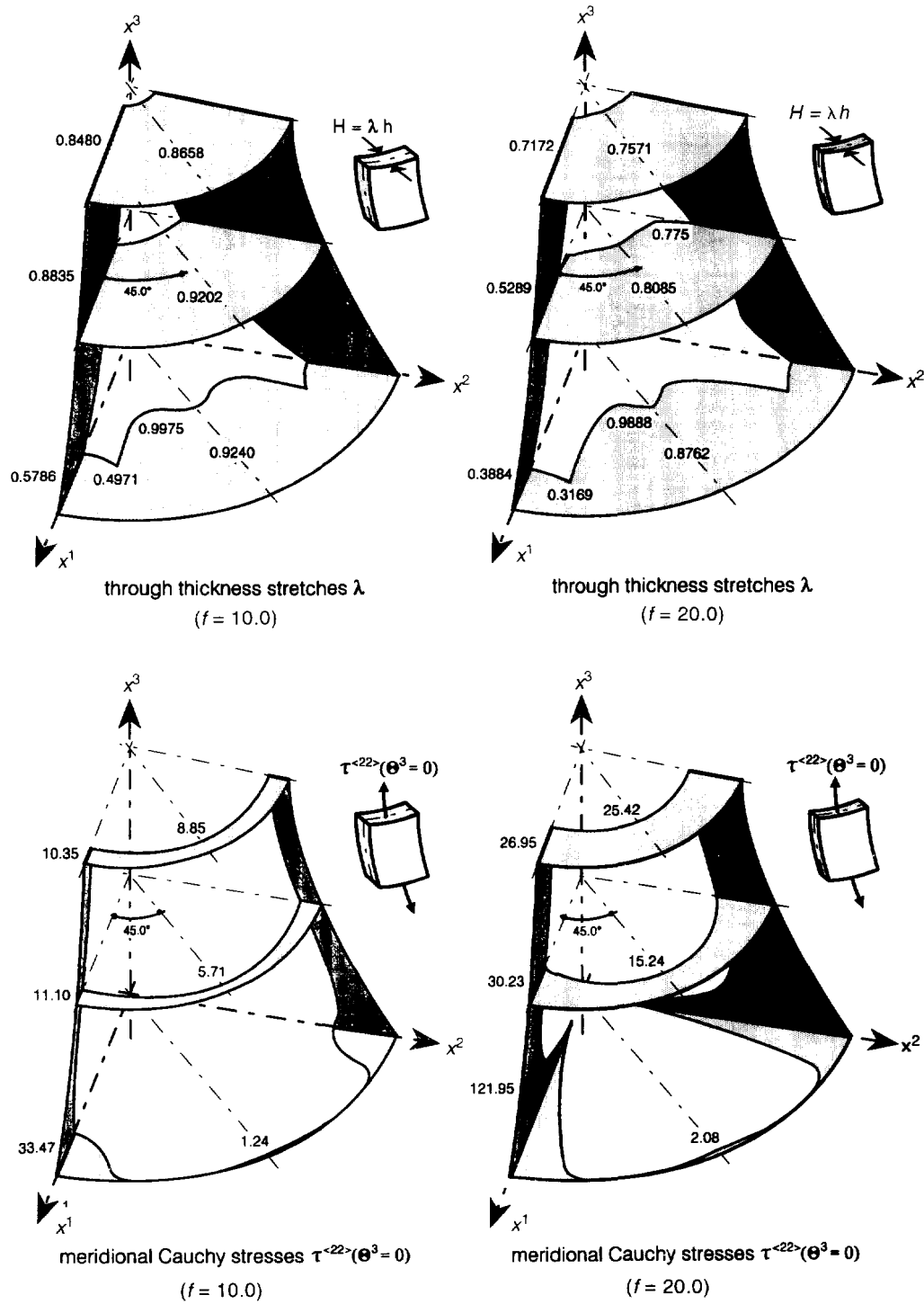


Fig. 11. Hyperboloidal shell: distributions of the stresses  $\tau^{<22>}(\theta^3 = 0)$  and the thickness stretching parameter  $\lambda$ .

for higher load level which confirms the significant role of transverse normal strains in the large strain analysis.

### 11. CONCLUSIONS

In the present study a general applicable kinematic model has been presented for large-strain and finite-rotation analysis of arbitrary shell structures. This model has then been

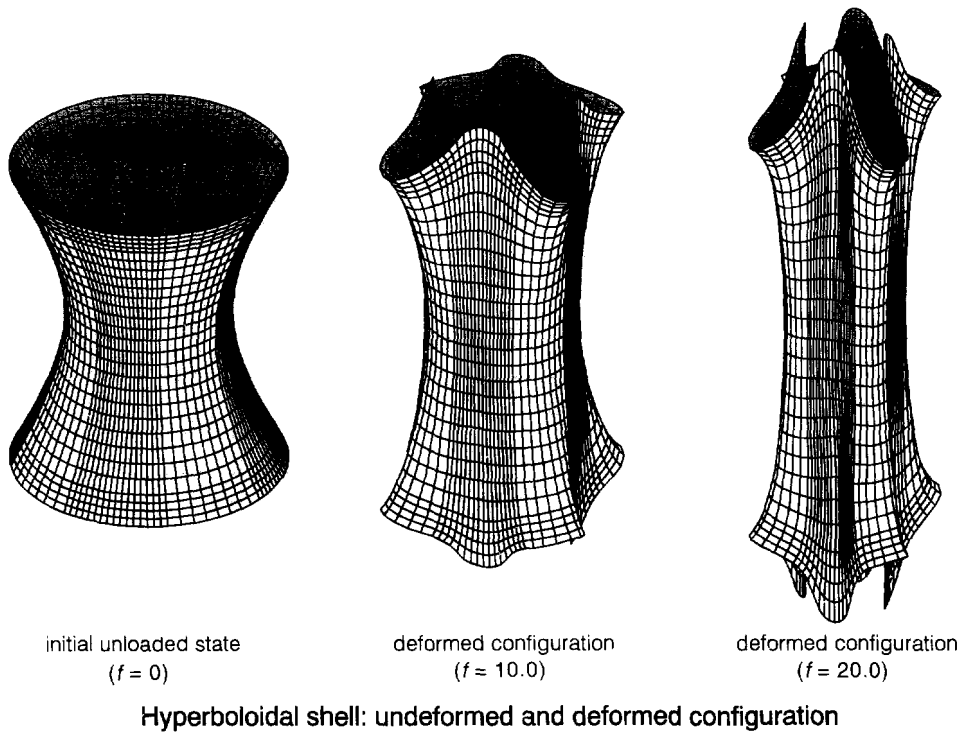


Fig. 12. Hyperboloidal shell: undeformed and deformed configurations.

coupled with the strain energy density of rubber-like materials and transformed into an isoparametric four-node finite element. By means of extended numerical studies achieved by this model we may state the following concerning different aspects.

#### 11.1. Theoretical formulation

- The kinematic model proposed enables to consider compressible and incompressible shells within a unified formulation. In the present study the performance of this model is demonstrated on the example of rubber-like components characterized by incompressibility. Its suitability for the analysis of compressible shells has been however shown in an earlier study [Başar and Ding (1994)] on the example of composites. This model involves a number of simplified models (see Section 3) which provides a great flexibility in large-strain analysis.
- No numerical difficulties have been observed due to the inclusion of the incompressible condition. On the contrary this constraint renders the transverse normal strains numerically stable and thus the analysis can be carried out by means of a linear kinematic model. In dealing with compressible materials the kinematic model should however involve at least a quadratic stretching parameter to ensure numerical stability unless another stabilisation procedure e.g. enhanced FE-formulation [Büchter *et al.* (1994)] is adopted.
- The accuracy of numerical results produced for stresses have been checked on a number of simple examples with available analytical solutions. Finite element formulations available in literature mostly present numerical results for displacements but not for stresses. Accordingly, in dealing with complex examples corresponding results could be checked only in some cases through global equilibrium considerations.

#### 11.2. FE-formulation

- Finite element developed is lock-free, insensitive to shape distortions and able to deal with arbitrarily strong nonlinear situations. Deformations connected with very large thickness changes and rotations could be analysed even on complex geometries without numerical difficulties.

- For infinitesimal strains and for Poisson's ratio  $\nu = 0.5$  the present material model reduces to the classical Hookean model. Large strain analysis can however hardly be achieved by means of classical finite-rotation models [Başar and Ding (1990); Başar *et al.* (1992)] on the basis of a Hookean material model.
- On the examples investigated up to now with thickness to length ratios  $h/L < 1/10$  no significant discrepancies have been observed between the results of the present model and those produced by its Kirchhoff–Love type counterparts [Başar and Ding (1996)]. We however find the present model more advantageous since it can easily be extended to multilayer-models (layerwise model) which have been proved to achieve arbitrarily accurate results even for extremely unfavourable conditions, e.g. 3D structures [Başar *et al.* (1993)]. This advantage is evidently due to transverse shear strains involved in the present model while Kirchhoff–Love type models are in this sense not predictive at all.

*Acknowledgement*—The present study is supported by a research grant of the German National Science Foundation (DFG) under Ba969.3-1. This support is gratefully acknowledged.

#### REFERENCES

- Başar, Y. and Ding, Y. (1990). Finite-rotation elements for the nonlinear analysis of thin shell structures. *International Journal of Solids and Structures* **26**, 83–97.
- Başar, Y. and Ding, Y. (1994). The consideration of transverse normal strains in the finite-rotation shell analysis. *2nd Biennial European Joint Conference on Engineering Systems, Design and Analysis*, Queen Mary & Westfield College, University of London, July 4–7, 1994.
- Başar, Y. and Ding, Y. (1995). Interlaminar stress analysis of composites: layerwise shell finite elements including transverse strains. *Composite Engineering* **5**, 485–499.
- Başar, Y. and Ding, Y. (1996). Finite-element analysis of hyperelastic thin shells with large strains. Submitted to *Computational Mechanics*.
- Başar, Y., Ding, Y. and Krätzig, W. B. (1992). Finite-rotation shell elements via mixed formulation. *Computational Mechanics* **10**, 289–306.
- Başar, Y., Ding, Y. and Schultz, R. (1993). Refined shear-deformation models for composite laminates with finite rotations. *International Journal of Solids and Structures* **30**, 2611–2638.
- Başar, Y. and Krätzig, W. B. (1985). *Mechanik der Flächentragwerke*. Friedr. Vieweg und Sohn, Braunschweig, Wiesbaden.
- Büchter, N. and Ramm, E. (1992). Shell theory versus degeneration—a comparison in large rotation finite element analysis. *International Journal of Numerical Methods in Engineering* **34**, 39–59.
- Büchter, N., Ramm, E. and Roehl, D. (1994). Three-dimensional extension of nonlinear shell formulation based on the enhanced assumed strain concept. *International Journal of Numerical Methods in Engineering* **37**, 2551–2568.
- Dvorkin, E. N. and Bathe, K.-J. (1984). A continuum mechanics based four-node shell element for general nonlinear analysis. *Engineering Computing* **1**, 77–88.
- Fox, D. D. and Simo, J. C. (1992). A drill rotation formulation for geometrically exact shells. *Computer Methods in Applied Mechanical Engineering* **98**, 329–343.
- Gebhardt, H. (1990). *Finite Element Konzepte für schubelastische Schalen mit endlichen Drehungen*. Schriftreihe Heft 10. Karlsruhe 1990. Institut für Baustatik, Universität Fridericiana Karlsruhe (TH), Herausgeber: U. Vogel, K. Schweizerhof.
- Green, A. E. and Zerna, W. (1968). *Theoretical Elasticity*, 2nd edn. Clarendon Press, Oxford.
- Gruttmann, F., Stein, E. and Wriggers, P. (1989). Theory and numerics of thin elastic shells with finite rotations. *Ing. Archiv*, **59**, 54–67.
- Gruttmann, F. and Taylor, R. L. (1992). Theory and finite element formulation of rubberlike membrane shells using principal stretches. *International Journal of Numerical Methods in Engineering* **35**, 1111–1126.
- Hart-Smith, L. J. and Crisp, J. D. C. (1967). Large elastic deformations of thin rubber membranes. *International Journal of Engineering Science* **5**, 1–24.
- Ibrahimbegovic, A. and Frey, F. (1994). Stress resultant geometrically non-linear shell theory with drilling rotations, part III: linearized kinematics. *International Journal of Numerical Methods in Engineering* **37**, 3659–3683.
- Kühlhorn, A. and Schoop, H. (1992). A nonlinear theory of sandwich shells including the wrinkling phenomenon. *Archives of Applied Mechanics* **62**, 413–427.
- Lo, K. H., Christensen, R. M. and Wu, E. M. (1977). A higher-order theory of plate deformation, part 2: laminated plates. *Journal of Applied Mechanics ASME* **44**, 663–676.
- Makowski, J. and Stumpf, H. (1989). Finite axisymmetric deformation of shells of revolution with application to flexural buckling of circular plates. *Ing. Arch.* **59**, 456–472.
- Parisch, H. (1986). Efficient non-linear finite element shell formulation involving large strains. *Engineering Computing* **3**, 125–128.
- Ramm, E. (1976). *Geometrisch nichtlineare Elastostatik und Finite Elemente*. Habilitationsschrift Bericht Nr. 76-2. Institut für Baustatik der Universität Stuttgart.
- Sansour, C. (1995). A theory and finite element formulation of shells at finite deformations involving thickness change: circumventing the use of a rotation tensor. *Archives of Applied Mechanics* **65**, 194–216.

Sansour, C. and Bufler, H. (1992). An exact finite rotation shell theory, its mixed variational formulation and its finite element implementation. *International Journal of Numerical Methods in Engineering* **34**, 73–115.

Schieck, B. (1989). Große elastische Dehnungen in Schalen aus hyperelastischen inkompressiblen Materialien. Mitt. Inst. f. Mech. Nr. 69, Ruhr-Universität Bochum, Germany.

Schieck, B., Pietraszkiewicz, W. and Stumpf, H. (1992). Theory and numerical analysis of shells undergoing large elastic strains. *International Journal of Solids and Structures* **29**, 689–709.

Simmonds, J. G. (1986). The strain energy density of rubber-like shells of revolution undergoing torsionless, axisymmetric deformations (axisshells). *Journal of Applied Mechanics* **53**, 593–596.

Simo, J. C. (1993). On a stress resultant geometrically exact shell model, Part VII: shell intersections with 5/6 DOF finite element formulations. *Computer Methods in Applied Mechanical Engineering* **108**, 319–339.

Simo, J. C., Fox, D. D. and Rifai, M. S. (1989). On a stress resultant geometrically exact shell model, Part II: the linear theory; computational aspects. *Computer Methods in Applied Mechanical Engineering* **73**, 53–92.

Simo, J. C., Fox, D. D. and Rifai, M. S. (1990a). On a stress resultant geometrically exact shell model, Part III: computational aspects of the nonlinear theory. *Computer Methods in Applied Mechanical Engineering* **79**, 21–70.

Simo, J. C., Rifai, M. S. and Fox, D. D. (1990b). On a stress resultant geometrically exact shell model, Part IV: variable thickness with through-the-thickness stretching. *Computer Methods in Applied Mechanical Engineering* **81**, 91–126.

Taber, L. A. (1985). On approximate large strain relations for a shell of revolution. *International Journal of Non-Linear Mechanics* **20**, 27–39.

Wriggers, P. and Taylor, R. L. (1990). A fully non-linear axisymmetrical membrane element for rubber-like materials. *Engineering Computing* **7**, 303–310.

APPENDIX I

Abbreviations used for strain invariants and internal potential energy

Strain invariants

$$\begin{aligned}
 I_1 &= 3 + A + 2\gamma_3^2, & I_2 &= 3 + 2A + 4D + 2\gamma_3^2(2 + A) - 4Q. \\
 I_3 &= (1 + 2\gamma_3)(1 + N) + S \\
 A &= 2\gamma_2^2 = \overset{0}{A} + \theta^3 \overset{1}{A} + (\theta^3)^2 \overset{2}{A} \\
 \overset{0}{A} &= 2\gamma_2^0 \gamma_2^0, & \overset{1}{A} &= 2\hat{e}_2^2 = 2(\gamma_2^1 \gamma_2^0 + 2b_{\beta}^{\gamma} \frac{\overset{0}{\gamma}_2^0}{\gamma_2^0}), & \overset{2}{A} &= 2\hat{e}_2^2 = 2(\gamma_2^2 \gamma_2^0 + 2b_{\beta}^{\gamma} \frac{\overset{1}{\gamma}_2^0}{\gamma_2^0} + 3b_{\beta}^{\gamma} b_{\beta}^{\delta} \frac{\overset{0}{\gamma}_2^0}{\gamma_2^0}) \\
 D &= \frac{1}{2}(\gamma_2^1 \gamma_2^0 - \gamma_2^0 \gamma_2^1) = \overset{0}{D} + \theta^3 \overset{1}{D} + (\theta^3)^2 \overset{2}{D} + \dots \\
 \overset{0}{D} &= \frac{1}{2}(\gamma_2^0 \gamma_2^0 - \gamma_2^0 \gamma_2^0), & \overset{1}{D} &= \frac{0}{\gamma_2} \frac{1}{\beta} \frac{0}{\beta} - \frac{0}{\gamma_2} \frac{1}{\beta} \frac{0}{\beta}, & \overset{2}{D} &= \frac{0}{\gamma_2} \frac{2}{\beta} \frac{0}{\beta} - \frac{0}{\gamma_2} \frac{2}{\beta} \frac{0}{\beta} + \frac{1}{2}(\hat{e}_2^1 \frac{1}{\beta} - \frac{1}{\beta} \hat{e}_2^1) \\
 N &= A + 4D = \overset{0}{N} + \theta^3 \overset{1}{N} + (\theta^3)^2 \overset{2}{N} + \dots, & \overset{0}{N} &= \overset{0}{A} + 4\overset{0}{D} \\
 Q &= \gamma_2^1 \gamma_3^2 = \overset{0}{Q} + \theta^3 \overset{1}{Q} + (\theta^3)^2 \overset{2}{Q} \\
 \overset{0}{Q} &= \frac{0}{\gamma_2} \frac{0}{\gamma_3}, & \overset{1}{Q} &= 2(\frac{0}{\gamma_2} \frac{1}{\gamma_3} + b_{\beta}^{\gamma} \frac{\overset{0}{\gamma}_2^0}{\gamma_2^0} \frac{\overset{0}{\gamma}_3^0}{\gamma_3^0}), & \overset{2}{Q} &= \frac{1}{\gamma_2} \frac{1}{\gamma_3} + 2b_{\beta}^{\gamma} \frac{\overset{0}{\gamma}_2^0}{\gamma_2^0} \frac{\overset{1}{\gamma}_3^0}{\gamma_3^0} \\
 S &= -4[\gamma_2^1 \gamma_3^2 - 2\gamma_2^2(\gamma_{\beta 3}^0 \gamma_2^0 - \gamma_{\beta 3}^0 \gamma_2^0)] = \overset{0}{S} + \theta^3 \overset{1}{S} + (\theta^3)^2 \overset{2}{S} + \dots \\
 \overset{0}{S} &= 4\gamma_2^0 \gamma_3^0 [2(\frac{0}{\gamma_2} \frac{0}{\gamma_3} - \frac{0}{\gamma_2} \frac{0}{\gamma_3}) - \frac{0}{\gamma_2} \frac{0}{\gamma_3}] \\
 \overset{1}{S} &= 4\gamma_2^0 \gamma_3^0 [2(\frac{0}{\gamma_2} \frac{1}{\gamma_3} + \frac{1}{\beta} \frac{0}{\beta} - \frac{0}{\gamma_2} \frac{1}{\gamma_3} - \frac{1}{\beta} \frac{0}{\beta}) - \frac{1}{\gamma_2} \frac{0}{\gamma_3}] \\
 &\quad + 4(\frac{1}{\gamma_2} + 2b_{\beta}^{\gamma} \frac{\overset{0}{\gamma}_2^0}{\gamma_2^0}) [2(\frac{0}{\gamma_2} \frac{0}{\gamma_3} - \frac{0}{\gamma_2} \frac{0}{\gamma_3}) - \frac{0}{\gamma_2} \frac{0}{\gamma_3}] \\
 \overset{2}{S} &= 8\gamma_2^0 \gamma_3^0 (\hat{e}_2^1 \frac{0}{\gamma_3} + \frac{1}{\beta} \frac{0}{\beta} - \frac{2}{\beta} \frac{0}{\beta} - \frac{1}{\beta} \frac{1}{\gamma_3}) \\
 &\quad + 4(\frac{1}{\gamma_2} + 2b_{\beta}^{\gamma} \frac{\overset{0}{\gamma}_2^0}{\gamma_2^0}) [2(\frac{0}{\gamma_2} \frac{1}{\gamma_3} + \frac{1}{\beta} \frac{0}{\beta} - \frac{0}{\gamma_2} \frac{1}{\gamma_3} - \frac{1}{\beta} \frac{0}{\beta}) - \frac{1}{\gamma_2} \frac{0}{\gamma_3}] \\
 R &= \frac{S + N}{1 + N} \\
 \overset{0}{R} &= \frac{\overset{0}{S} + \overset{0}{N}}{1 + \overset{0}{N}}, & \overset{1}{R} &= \frac{\overset{1}{S}}{1 + \overset{0}{N}} + \frac{(1 - \overset{0}{S}) \overset{1}{N}}{(1 + \overset{0}{N})^2} \\
 \overset{2}{R} &= \frac{\overset{2}{S}}{1 + \overset{0}{N}} + \frac{(1 - \overset{0}{S}) \overset{2}{N} - \overset{1}{N} \overset{1}{S}}{(1 + \overset{0}{N})^2} - \frac{(1 - \overset{0}{S}) (\overset{1}{N})^2}{(1 + \overset{0}{N})^3}
 \end{aligned}$$

( ) : terms to be neglected for thin shells.

APPENDIX 2

*Incremental variables used in the nonlinear analysis*

$$\begin{aligned} \bar{\pi}_0 &= c_1(\bar{A} - \bar{R}) + c_2[(2 - \bar{R})\bar{A} + 4\bar{D} - (2 + \bar{A})\bar{R} - 4\bar{Q}] \\ \bar{\pi}_1 &= c_1(\bar{A} - \bar{R}) + c_2[(2 - \bar{R})\bar{A} + 4\bar{D} - (2 + \bar{A})\bar{R} - 4\bar{Q} - 2\bar{A}\bar{R}] \\ \bar{\pi}_2 &= c_1(\bar{A} - \bar{R}) + c_2[(2 - \bar{R})\bar{A} + 4\bar{D} - (2 + \bar{A})\bar{R} - \bar{A}\bar{R} - \bar{R}\bar{A} - 4\bar{Q} - \bar{A}\bar{R} - \bar{R}\bar{A}] \\ \bar{\pi}_3 &= c_1(\bar{A} - \bar{R}) + c_2[(2 - \bar{R})\bar{A} + 4\bar{D} - (2 + \bar{A})\bar{R} - \bar{A}\bar{R} - \bar{R}\bar{A} - 4\bar{Q} - \bar{A}\bar{R} \\ &\quad - \bar{R}\bar{A} - 2\bar{A}\bar{R} - 2\bar{A}\bar{R} - 2\bar{A}\bar{R}] \\ \bar{A} &= 2\bar{\gamma}_z^{\bar{z}}, \quad \bar{A} = 2\bar{\gamma}_z^{\bar{z}} \\ \bar{A} &= 2(\bar{\gamma}_z^{\bar{z}} + 2b_{\rho}^{\bar{z}} \bar{\gamma}_z^{\bar{z}}), \quad \bar{A} = 2(\bar{\gamma}_z^{\bar{z}} + 2b_{\rho}^{\bar{z}} \bar{\gamma}_z^{\bar{z}}) \\ \bar{A} &= 2(\bar{\gamma}_z^{\bar{z}} + 2b_{\rho}^{\bar{z}} \bar{\gamma}_z^{\bar{z}} + 3b_{\rho}^{\bar{z}} b_{\rho}^{\bar{z}} \bar{\gamma}_z^{\bar{z}}) \\ \bar{A} &= 2(\bar{\gamma}_z^{\bar{z}} + 2b_{\rho}^{\bar{z}} \bar{\gamma}_z^{\bar{z}} + 3b_{\rho}^{\bar{z}} b_{\rho}^{\bar{z}} \bar{\gamma}_z^{\bar{z}}) \\ \bar{D} &= \bar{\gamma}_z^{\bar{z}} \bar{\gamma}_z^{\bar{z}} - \bar{\gamma}_z^{\bar{z}} \bar{\gamma}_z^{\bar{z}} \\ \bar{D} &= \bar{\gamma}_z^{\bar{z}} \bar{\gamma}_z^{\bar{z}} - \bar{\gamma}_z^{\bar{z}} \bar{\gamma}_z^{\bar{z}} + \bar{\gamma}_z^{\bar{z}} \bar{\gamma}_z^{\bar{z}} - \bar{\gamma}_z^{\bar{z}} \bar{\gamma}_z^{\bar{z}} \\ \bar{D} &= \bar{\gamma}_z^{\bar{z}} \bar{\gamma}_z^{\bar{z}} + \bar{\gamma}_z^{\bar{z}} \bar{\gamma}_z^{\bar{z}} - \bar{\gamma}_z^{\bar{z}} \bar{\gamma}_z^{\bar{z}} - \bar{\gamma}_z^{\bar{z}} \bar{\gamma}_z^{\bar{z}} \\ \bar{D} &= \bar{\gamma}_z^{\bar{z}} \bar{\gamma}_z^{\bar{z}} + \bar{\gamma}_z^{\bar{z}} \bar{\gamma}_z^{\bar{z}} - \bar{\gamma}_z^{\bar{z}} \bar{\gamma}_z^{\bar{z}} - \bar{\gamma}_z^{\bar{z}} \bar{\gamma}_z^{\bar{z}} + 2\bar{\gamma}_z^{\bar{z}} \bar{\gamma}_z^{\bar{z}} - 2\bar{\gamma}_z^{\bar{z}} \bar{\gamma}_z^{\bar{z}} \\ \bar{D} &= \bar{\gamma}_z^{\bar{z}} \bar{\gamma}_z^{\bar{z}} + \bar{\gamma}_z^{\bar{z}} \bar{\gamma}_z^{\bar{z}} - \bar{\gamma}_z^{\bar{z}} \bar{\gamma}_z^{\bar{z}} - \bar{\gamma}_z^{\bar{z}} \bar{\gamma}_z^{\bar{z}} + \bar{\gamma}_z^{\bar{z}} \bar{\gamma}_z^{\bar{z}} - \bar{\gamma}_z^{\bar{z}} \bar{\gamma}_z^{\bar{z}} \\ \bar{D} &= \bar{\gamma}_z^{\bar{z}} \bar{\gamma}_z^{\bar{z}} + \bar{\gamma}_z^{\bar{z}} \bar{\gamma}_z^{\bar{z}} - \bar{\gamma}_z^{\bar{z}} \bar{\gamma}_z^{\bar{z}} - \bar{\gamma}_z^{\bar{z}} \bar{\gamma}_z^{\bar{z}} + \bar{\gamma}_z^{\bar{z}} \bar{\gamma}_z^{\bar{z}} - \bar{\gamma}_z^{\bar{z}} \bar{\gamma}_z^{\bar{z}} + \bar{\gamma}_z^{\bar{z}} \bar{\gamma}_z^{\bar{z}} - \bar{\gamma}_z^{\bar{z}} \bar{\gamma}_z^{\bar{z}} \\ \bar{N} &= \bar{A} + 4\bar{D}, \quad \bar{N} = \bar{A} + 4\bar{D} \\ \bar{Q} &= 2\bar{\gamma}_z^{\bar{z}} \bar{\gamma}_z^{\bar{z}}, \quad \bar{Q} = 2\bar{\gamma}_z^{\bar{z}} \bar{\gamma}_z^{\bar{z}} + 2\bar{\gamma}_z^{\bar{z}} \bar{\gamma}_z^{\bar{z}} \\ \bar{Q} &= 2(\bar{\gamma}_z^{\bar{z}} \bar{\gamma}_z^{\bar{z}} + \bar{\gamma}_z^{\bar{z}} \bar{\gamma}_z^{\bar{z}} + 2b_{\rho}^{\bar{z}} \bar{\gamma}_z^{\bar{z}} \bar{\gamma}_z^{\bar{z}}) \\ \bar{Q} &= 2(\bar{\gamma}_z^{\bar{z}} \bar{\gamma}_z^{\bar{z}} + \bar{\gamma}_z^{\bar{z}} \bar{\gamma}_z^{\bar{z}} + 2b_{\rho}^{\bar{z}} \bar{\gamma}_z^{\bar{z}} \bar{\gamma}_z^{\bar{z}} + 2\bar{\gamma}_z^{\bar{z}} \bar{\gamma}_z^{\bar{z}} + 2b_{\rho}^{\bar{z}} \bar{\gamma}_z^{\bar{z}} \bar{\gamma}_z^{\bar{z}}) \\ \bar{Q} &= 2\bar{\gamma}_z^{\bar{z}} \bar{\gamma}_z^{\bar{z}} + 2b_{\rho}^{\bar{z}} (\bar{\gamma}_z^{\bar{z}} \bar{\gamma}_z^{\bar{z}} + \bar{\gamma}_z^{\bar{z}} \bar{\gamma}_z^{\bar{z}}) \\ \bar{Q} &= 2(\bar{\gamma}_z^{\bar{z}} \bar{\gamma}_z^{\bar{z}} + 2b_{\rho}^{\bar{z}} (\bar{\gamma}_z^{\bar{z}} \bar{\gamma}_z^{\bar{z}} + \bar{\gamma}_z^{\bar{z}} \bar{\gamma}_z^{\bar{z}}) + 2\bar{\gamma}_z^{\bar{z}} \bar{\gamma}_z^{\bar{z}} + 4b_{\rho}^{\bar{z}} \bar{\gamma}_z^{\bar{z}} \bar{\gamma}_z^{\bar{z}}) \end{aligned}$$

( $\bar{\quad}$ ): terms to be neglected for thin shells.